

ChemComm

Accepted Manuscript



This is an *Accepted Manuscript*, which has been through the Royal Society of Chemistry peer review process and has been accepted for publication.

Accepted Manuscripts are published online shortly after acceptance, before technical editing, formatting and proof reading. Using this free service, authors can make their results available to the community, in citable form, before we publish the edited article. We will replace this *Accepted Manuscript* with the edited and formatted *Advance Article* as soon as it is available.

You can find more information about *Accepted Manuscripts* in the [Information for Authors](#).

Please note that technical editing may introduce minor changes to the text and/or graphics, which may alter content. The journal's standard [Terms & Conditions](#) and the [Ethical guidelines](#) still apply. In no event shall the Royal Society of Chemistry be held responsible for any errors or omissions in this *Accepted Manuscript* or any consequences arising from the use of any information it contains.



Journal Name

COMMUNICATION

The synthesis and evaluation of near-infrared probes with barbituric acid acceptors for *in vivo* detection of amyloid plaques

Received 00th January 20xx,
Accepted 00th January 20xx

Kaixiang Zhou,^a Hualong Fu,^a Liang Feng,^a Mengchao Cui,^{*a} Jiawei Dai^b and Boli Liu^a

DOI: 10.1039/x0xx00000x

www.rsc.org/

A new array of near-infrared probes containing barbituric acid acceptors has been developed as A β imaging agents. These probes displayed long-emission wavelengths and large Stokes shifts, as well as a high affinity for A β aggregates. *In vivo* and *ex vivo* studies demonstrated that BBTOM-3 could intensely label A β plaques in the brains of transgenic mice.

Alzheimer's disease (AD) is a neurodegenerative and lethal disorder that leads to memory impairments and cognitive defects. Amyloid cascade hypothesis is accepted as the main nosogenesis of AD, which suggests that A β deposits in the brain is a good biomarker for diagnosis of AD.¹⁻⁴ However, early non-invasive detection *in vivo* still presents a challenge. To address this problem, different imaging techniques, such as single-photon emission-computed tomography (SPECT)^{5, 6}, positron emission computed tomography (PET)⁷, magnetic resonance imaging (MRI)⁸ and optical imaging⁹ have been employed for this purpose.

In addition to such radiation-based imaging techniques as PET and SPECT, optical imaging is one of the most attractive imaging modalities in research and clinical practice that possesses the advantages of ease of operation, rapid detection and prevention of exposure to radiation. To obtain an acceptable penetration depth and avoid the auto-fluorescence of biological matter, long-wavelength detection methods using near-infrared (NIR) fluorescent probes are very beneficial^{10, 11}. The probes in the NIR spectral range targeting A β deposits in the brain have been exploited including AOI-987¹², NIAD-4¹³, CRANAD-2¹⁴ and THK-265¹⁵. As the first optimal NIR fluorescent probe targeting A β aggregates, the charged oxazine derivative AOI-987 has some unfavorable properties, such as a narrow Stokes shift and only

moderate affinity. The emission maximum of the highly polarizable bithiophene derivative NIAD-4 is not in the NIR range. The difluoroboronate curcumin derivative CRANAD-2 is restricted by a slow clearance rate from the normal brain. THK-265, containing two thiobarbituric acid acceptors, has moderate affinity for A β aggregates, narrow Stokes shift and poor BBB penetration, which limits its further application in NIR imaging.

Recently, our group reported a series of smart A β probes for NIR imaging based on the pull-push architecture with electron donating and withdrawing moieties bridged by the π -conjugated system consisting of polyenic chains. Several electron acceptors such as malononitrile, Meldrum's acid, dimedone, methyl cyanoacetate and dimethyl malonate were applied to our NIR probes (Fig 1). Among them, DANIR-2c and MCAAD-3 with coplanar geometries displayed sufficient affinity and excellent *in vivo* NIR imaging,^{16, 17} while the probes containing nonplanar acceptors (MAAD-3 and DMDAD-3) displayed decreased binding affinity and poor brain uptake. We reasonably believed that the coplanar geometry of a probe is crucial for A β binding. In addition to this, the emission maximum of these probes upon binding to A β plaques is under 650 nm which is not within the "window" (650 - 900 nm). Hence, we employed the planar barbituric acid moieties as stronger acceptors to obtain a greater affinity and longer emission wavelength.¹⁸ Herein, we reported the synthesis and biological evaluation of novel near-infrared probes with barbituric acid acceptors for the detection of A β plaques in the brains exhibiting AD.

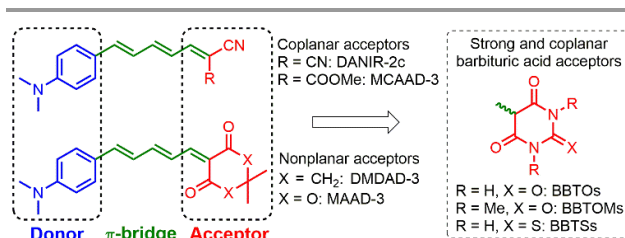
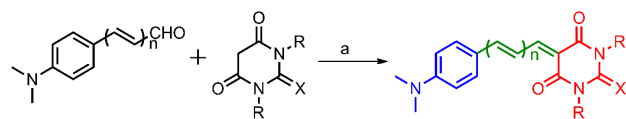


Fig. 1 Smart A β probes for NIR imaging based on the pull-push architecture with different acceptors.

^aKey Laboratory of Radiopharmaceuticals, Ministry of Education, College of Chemistry, Beijing Normal University, Beijing 100875, P. R. China. E-mail: cmc@bnu.edu.cn.

^bWuhan Institute for Neuroscience and Neuroengineering, South-Central University for Nationalities, Wuhan 430074, P. R. China.

† Electronic Supplementary Information (ESI) available: [Experimental details, absorption and fluorescence spectra, ¹H-NMR, ¹³C-NMR, MS and HRMS spectra were included here]. See DOI: 10.1039/x0xx00000x



Compounds	n	R	X	Compounds	n	R	X
BBTO-1	0	H	O	BBTOM-1	0	Me	O
BBTO-2	1	H	O	BBTOM-2	1	Me	O
BBTO-3	2	H	O	BBTOM-3	2	Me	O
BBTS-1	0	H	S	BBTOM-4	3	Me	O
BBTS-2	1	H	S	BBTOM-5	4	Me	O
BBTS-3	2	H	S				

Scheme 1 General synthetic routes of the NIR probes. (a) piperidine or K_2CO_3 as base, EtOH or DMF as solvent, r.t.

As shown in Scheme 1. The final NIR probes were prepared by Knoevenagel condensation from the appropriate aldehydes and barbituric acid derivatives as crystals with high yield and high purity (>95%, Fig S1). At first, the photophysical properties of the probes, including absorption and emission spectra in different solvents, extinction coefficients and quantum yield were determined. As shown in Table 1 and Table S1-2 (ESI[†]), lengthening the polyenic chains leads to an obvious redshift of the emission maxima and apparent solvatochromism with increasing solvent polarity. The emission maxima of probes with longer polyenic chains ($n \geq 3$) were successfully pushed into the NIR "window" in PBS (721 - 829 nm). In addition, these probes showed perfect Stokes shift (37 - 182 nm) which is favorable for *in vivo* NIR imaging.

Table 1 Selected spectroscopic and binding data for the synthesized NIRFs.

Probes	K_i (nM) ^a	$\Phi/\%$ ^b	λ_{em1} (nm) ^b	λ_{em2} (nm) ^c	λ_{em3} (nm) ^d	Fold ^e
BBTOM-1	-	0.08	522	550	-	-
BBTOM-2	119.9 ± 22.3	4.64	598	630	606	3.2
BBTOM-3	13.7 ± 4.6	7.81	691	729	690	10.9
	23.9 ± 7.4 ^f				678 ^f	14.7 ^f
BBTOM-4	28.8 ± 9.3	1.64	788	823	793	8.6
BBTOM-5	21.3 ± 6.3	0.26	822	829	822	2.3
BBTO-1	333.1 ± 38.7	0.05	518	502	-	-
BBTO-2	165.2 ± 23.1	5.71	602	627	-	-
BBTO-3	22.1 ± 5.6	8.16	696	720	693	12.0
BBTS-1	-	0.79	546	502	-	-
BBTS-2	121.0 ± 16.7	5.93	632	649	-	-
BBTS-3	14.7 ± 8.4	6.77	727	727	691	7.8

^a Measured in triplicate with results given as the mean ± SD. ^b The emission maxima measured in dichloromethane. ^c The emission maxima measured in PBS. ^d The emission maxima measured in PBS upon binding to $A\beta_{1-42}$ aggregates. ^e The fold increase in the fluorescence intensity upon binding to $A\beta_{1-42}$ aggregates. ^f Upon binding to $A\beta_{1-40}$ aggregates.

To enhance the specific fluorescence signals, an ideal NIR $A\beta$ probe should intensely change its fluorescent properties upon interacting with $A\beta$ plaques, while having weak interaction with serum albumin. As shown in Fig 2, Fig S8-9 (ESI[†]) and Table 1, probes with longer polyenic chains ($n = 3$) showed apparent fluorescence intensity increase (8- to 15-fold) and significant hypsochromic shift (30 - 50 nm) in the presence of $A\beta_{1-42}$ aggregates or $A\beta_{1-40}$ aggregates, which could be explained by the fact that these probes may be inserted into the hydrophobic pocket of $A\beta$ aggregates with high affinity^{13, 15}. However, very weak fluorescence changes were

observed in the presence of bovine serum albumin (BSA) and $A\beta$ monomers. It should be noted that upon binding to $A\beta_{1-42}$ aggregates, the emission wavelength of BBTOM-3, BBTO-3 and BBTS-3 still fell in the NIR range (> 690 nm).

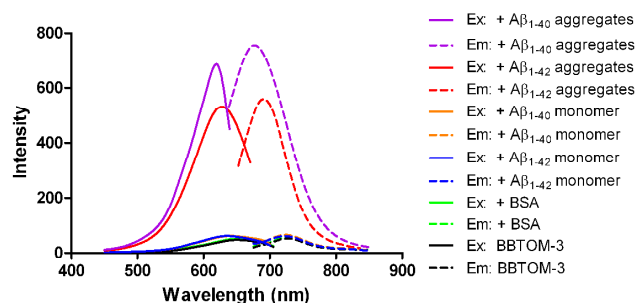


Fig. 2 The fluorescence spectra of the BBTOM-3 in PBS and in the presence of $A\beta$ aggregates, $A\beta$ monomers and BSA.

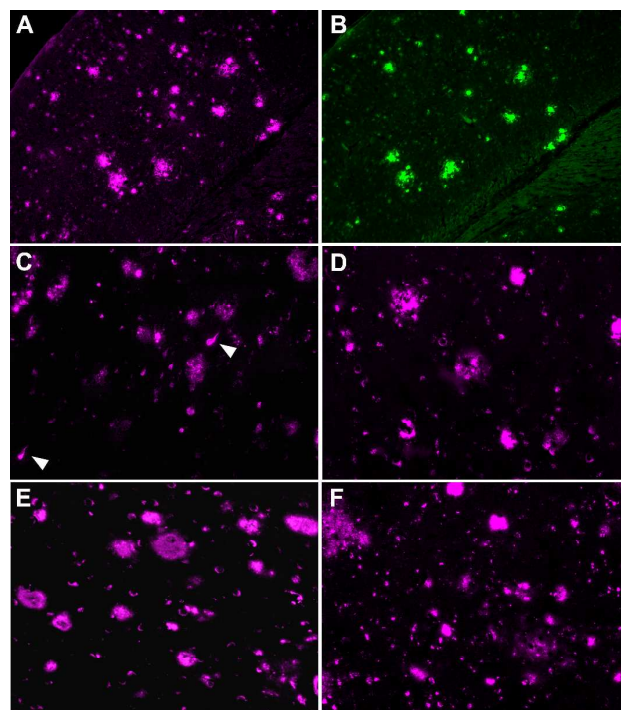


Fig. 3 Neuropathological staining with BBTOM-3 on brain slices from Tg mouse (C57BL6, APPswe/PSEN1, 12-months old, male) (A), the adjacent brain section was stained by Th-S (B). Fluorescence staining were also performed on brain tissues from AD patients (91-year old, male, temporal lobe) (C), (68-year old, female, temporal lobe) (D), (64-year old, female, temporal lobe) (E) and (70-year old, male, temporal lobe) (F). Arrow head indicate neurofibrillary tangles, magnification: 10 \times .

In vitro neuropathological fluorescence staining was then performed on brain slices from an APPswe/PSEN1 transgenic (Tg) mouse and AD patients ($n = 4$) to confirm the specific binding of these NIR probes to $A\beta$ plaques. As shown in Fig 3 and Fig S10-12 (ESI[†]), distinctive staining of $A\beta$ plaques was observed for all probes, and the results were in accordance with the staining of adjacent brain sections stained by Thioflavin-S (Th-S). As was anticipated, no obvious staining was observed on the brain slices

from the wild-type (WT) mouse or the healthy human (Fig S13-15 in the ESI[†]). Interestingly, similar to DANIR-2c, BBTOM-3 could also stain neurofibrillary tangles on the brain tissue of AD patients (Fig 3C, arrow head). The staining results indicate that these probes have specific binding to A β plaques. Next, competitive binding assays were performed to quantitatively evaluate the binding affinity of these probes to A β_{1-42} aggregates, [¹²⁵I]IMPY was used as the radioligand¹⁹. These probes inhibited the binding of [¹²⁵I]IMPY in a dose-dependent manner (Fig S16 in the ESI[†]), indicating that both the probe and [¹²⁵I]IMPY may share the same binding site on A β aggregates. As shown in Table 1, the binding affinity of these probes gradually increased with the extension of the polyenic chains. These results were consistent with the NIR probes containing other electron acceptors reported by our group, which imply that a certain length of conjugate structure is important for fitting into the binding pocket. Among them, BBTOM-3 displayed the highest binding affinity ($K_i = 13.7$ nM for A β_{1-42} aggregates and $K_i = 23.9$ nM for A β_{1-40} aggregates), which was higher than that of DANIR-2c ($K_i = 36.9$ nM)¹⁵ and MCAAD-3 ($K_i = 106$ nM) and much higher than that of MAAD-3 ($K_i = 354.3$ nM) and DMDAD-3 ($K_i = 645.2$ nM)¹⁶ containing nonplanar acceptors. This result indicates that the planar barbituric acid acceptor makes a significant contribution to the binding affinity. Due to its high binding affinity and appropriate emission wavelength upon binding to A β aggregates, BBTOM-3 was selected for further evaluations.

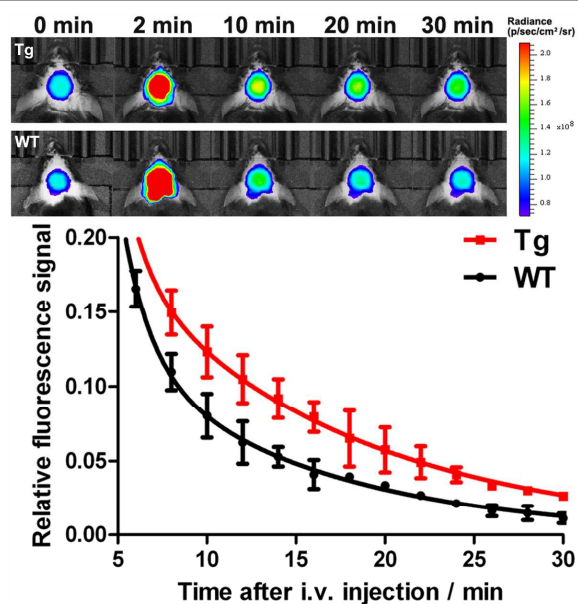


Fig. 4 *In vivo* NIR brain imaging of Tg and WT mice at different time points before and after i.v. injection of BBTOM-3. Brain kinetic curves of BBTOM-3 (left Y axis) and the values of $F(\text{Tg})/F(\text{WT})$ at selected time points (right Y axis).

To test the blood-brain barrier (BBB) permeability of the probe, BBTOM-3 was intravenously (i.v.) injected into ICR mice, and the concentration of probe in the brain homogenate was analyzed by HPLC. Compared with THK-265 (0.04%ID/g at 2 min post-injection)¹⁴, BBTOM-3 displayed approximately 20-fold higher

brain uptake (0.83%ID/g at 2 min post-injection). To further assess the potential of BBTOM-3 as an NIR probe for *in vivo* detection of A β plaques, *in vivo* NIR imaging was performed in Tg and age-matched WT mice ($n = 3$). As shown in Fig 4, higher fluorescent signals were observed in the brains of the Tg group than in the WT group at later time points after i.v. injection of BBTOM-3. Subsequently *ex vivo* histology was conducted after *in vivo* imaging to confirm the binding of BBTOM-3 to A β plaques. A higher number of A β plaques in the cortex, hippocampus (Fig 5A) and cerebellum regions (Fig 5C) of the brain sections from the Tg mouse were observed and the presence of plaques was confirmed by co-staining with Th-S (Fig 5B, D), while the WT mouse brain showed very weak fluorescence signals (Fig S18 in the ESI[†]). Although the brain uptake of BBTOM-3 is approximately 10 times lower than the most useful PET amyloid probes, it could still enter the brain of Tg mice at a sufficient level and selectively label the A β plaques.

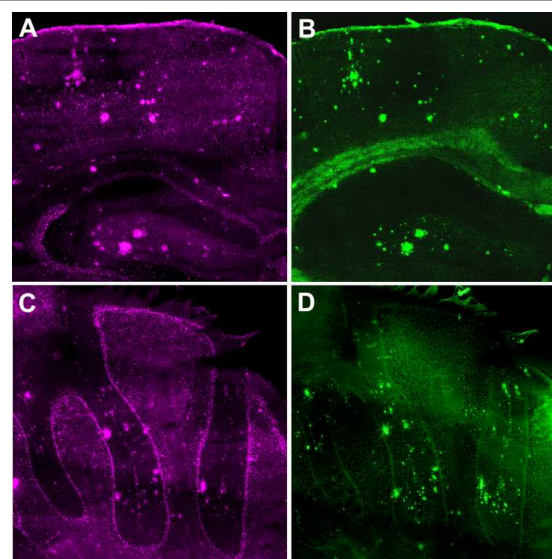


Fig. 5 *Ex vivo* histology observation of brain slices from a Tg mouse (C57BL6, APPsw/PSEN1, 12 months old, male) after intravenous administration of BBTOM-3. (A, in the cortex and hippocampus region, C, in the cerebellum region). The A β deposits were confirmed by staining with Th-S (B and D).

In summary, we successfully synthesized and evaluated an array of novel NIR A β plaque-specific fluorescence probes with planar barbituric acid as the acceptor. One of the probes, BBTOM-3 was stable towards photochemical isomerization and displayed excellent fluorescence properties and binding affinity upon binding to A β_{1-42} aggregates. Furthermore, after i.v. injection of BBTOM-3, a significant difference in the clearance profiles was observed between Tg and WT mice, and the specific plaque binding was further confirmed by *ex vivo* histology. From these results, we can conclude that BBTOM-3 is a novel promising NIR probe for the detection of A β deposition in the brain, even though further improvement should be implemented to enhance the BBB penetrating ability.

This work was funded by the National Nature Science Foundation of China (No. 21201019) and National Science and Technology Major Projects for Major New Drugs Innovation and Development

(no.2014ZX09507007-002). The authors thank Dr. Jin Liu (College of Life Science, Beijing Normal University) for assistance in the in vitro neuropathological staining.

Notes and references

1. J. Hardy and G. Higgins, *Science*, 1992, **256**, 184-185.
2. J. Hardy and D. J. Selkoe, *Science*, 2002, **297**, 353-356.
3. J. Hardy, *J. Alzheimers. Dis.*, 2006, **9**, 151-153.
4. H. F. Kung, *ACS Med. Chem. Lett.*, 2012, **3**, 265-267.
5. M. Ono and H. Saji, *Int. J. Mol. Imaging.*, 2011, **2011**, 543267.
6. M. Cui, *Curr. Med. Chem.*, 2014, **21**, 82-112.
7. C. C. Rowe and V. L. Villemagne, *J. Nucl. Med.*, 2011, **52**, 1733-1740.
8. Y. Z. Wadghiri, D. M. Hoang, T. Wisniewski and E. M. Sigurdsson, *Methods. Mol. Biol.*, 2012, **849**, 435-451.
9. M. Staderini, M. A. Martin, M. L. Bolognesi and J. C. Menendez, *Chem. Soc. Rev.*, 2015, **44**, 1807-1819.
10. V. Ntziachristos, J. Ripoll, L. V. Wang and R. Weissleder, *Nat. Biotechnol.*, 2005, **23**, 313-320.
11. V. Ntziachristos, *Annu. Rev. Biomed. Eng.*, 2006, **8**, 1-33.
12. M. Hintersteiner, A. Enz, P. Frey, A.-L. Jaton, W. Kinzy, R. Kneuer, U. Neumann, M. Rudin, M. Staufenbiel and M. Stoeckli, *Nat. Biotechnol.*, 2005, **23**, 577-583.
13. E. E. Nesterov, J. Skoch, B. T. Hyman, W. E. Klunk, B. J. Bacskai and T. M. Swager, *Angew. Chem.*, 2005, **44**, 5452-5456.
14. C. Ran, X. Xu, S. B. Raymond, B. J. Ferrara, K. Neal, B. J. Bacskai, Z. Medarova and A. Moore, *J. Am. Chem. Soc.*, 2009, **131**, 15257-15261.
15. N. Okamura, M. Mori, S. Furumoto, T. Yoshikawa, R. Harada, S. Ito, Y. Fujikawa, H. Arai, K. Yanai and Y. Kudo, *J. Alzheimers. Dis.*, 2011, **23**, 37-48.
16. M. Cui, M. Ono, H. Watanabe, H. Kimura, B. Liu and H. Saji, *J. Am. Chem. Soc.*, 2014, **136**, 3388-3394.
17. H. Fu, M. Cui, P. Tu, Z. Pan and B. Liu, *Chem. Commun.*, 2014, **50**, 11875-11878.
18. M. Klikar, F. Bureš, O. Pytela, T. Mikysek, Z. Padělková, A. Barsella, K. Dorkenoo and S. Achelle, *New. J. Chem.*, 2013, **37**, 4230-4240.
19. Z. P. Zhuang, M. P. Kung, A. Wilson, C. W. Lee, K. Plossl, C. Hou, D. M. Holtzman and H. F. Kung, *J. Med. Chem.*, 2003, **46**, 237-243.